XL CILAMCE
IBERO-LATIN AMERICAN CONGRESS ON COMPUTATIONAL METHODS IN ENGINEERING
NOVEMBER 11-14, 2019
Praiamar Natal Hotel & Convention
Natal, RN-BRAZIL

NUMERICAL SIMULATION OF CATHODIC PROTECTION SYSTEMS

Samuel B. Velten
samuelbv2004@yahoo.com.br
Department of Mechanics Engineering, IFES – Federal Institute of Espírito Santo
Morobá, CEP 29192-733, Aracruz, Espírito Santo, ES, Brazil
Edmundo G. de A. Costa
edmundo_costa@coc.ufrj.br
Department of Civil Engineering, COPPE – Federal University of Rio de Janeiro
Ilha do Fundão, CP 68506, CEP 21945-970, Rio de Janeiro, RJ, Brazil
Wilian J. dos Santos
wilianj@ufrrj.br
Department of Mathematics, Rural Federal University of Rio de Janeiro
Seropédica, CEP 23897-000, Rio de Janeiro, RJ, Brazil
José A. F. Santiago
José C. de F. Telles
santiago@coc.ufrj.br
telles@coc.ufrj.br
Department of Civil Engineering, COPPE – Federal University of Rio de Janeiro
Ilha do Fundão, CP 68506, CEP 21945-970, Rio de Janeiro, RJ, Brazil

Abstract. In this paper, the Method of Fundamental Solutions (MFS) and the Meshless Local Petrov-Galerkin (MLPG) method are applied to the numerical simulation of Cathodic Protection (CP) systems. The problem of CP systems is governed by the Laplace equation. In this problem, the boundary conditions are characterized by a nonlinear relationship between the electrochemical potential and the current density, called cathodic polarization curve. Thus, the Levenberg-Marquardt algorithm is here used to solve the nonlinear problem. The performance of both methods is evaluated by comparing its results with these provided by the Boundary Element Method (BEM). Furthermore, the BEM coupled with the Genetic Algorithms (GAs) is applied for the simulation of inverse problems in CP systems. The van Genuchten-Mualem model is here used to predict the parameters of the nonlinear polarization curve. A numerical simulation is presented in order to illustrate the good performance of the coupled BEM-GAs approach.

Keywords: Boundary Element Method, Method of Fundamental Solutions, Meshless Local Petrov-Galerkin Method, Cathodic protection systems, Genetic algorithms

1 Introduction

Corrosion is a spontaneous phenomenon that must be prevented or controlled, due to the high costs involved. To this end, cathodic protection techniques have been widely applied, including cases of buried pipelines, underground storage tanks and offshore structures. The technique aims to convert the metallic structure into a cathode of an electrochemical cell, delivering electrons for cathodic reactions [1]. Two alternatives are identifiable to produce the current density required to keep the electrochemical potential within the immunity to corrosion: galvanic and/or impressed current cathodic protection. In both cases, numerical simulations have been used to calculate the potential and current density distributions over the metal surface to be protected. The first numerical methods applied to corrosion problems, governed by well-known Laplace equation, were the finite difference method (FDM) [2, 3] and the finite element method (FEM) [4, 5]. However, the boundary element method (BEM) has been successfully used for many industrial applications [6, 7] and, nowadays, is the most popular solution technique for the study of corrosion engineering problems [8, 9, 10, 11].

In addition to BEM, there is also one more alternative technique with the same characteristics, in which no mesh or numerical integration processes are required: the method of fundamental solutions (MFS) [12]. With this in mind, Santos, Santiago and Telles [13] proposed the MFS to simulate cathodic protection systems with non-linear boundary conditions. In the cited paper, the intensities and positions of the virtual sources were successfully obtained with the usage of genetic algorithms (GAs). On top of that, other meshless techniques have appeared, such as a variant of the meshless local Petrov-Galerkin (MLPG) method, denoted as MLPG2 [14]. In the last decade, the MLPG methods are successfully used in a large number of applications [15, 16, 17], and the present authors believe that these truly meshless methods can also be applied to the simulation of cathodic protection problems. Hence, in this paper, the MLPG2 method is used as a possibility for CP numerical analysis.

The main purpose of this paper is to study numerical tools for the solution of direct and inverse corrosion problems. For direct problems, the MFS and MLPG2 methods are applied to simulate the potential distribution over the metal surface to be protected. In the inverse analysis, the BEM and the GAs are coupled in order to deal with the strong polarization of CP systems. The parameters of the polarization curve are provided by the van Genuchten-Mualem model and its parameters are compared with the values estimated by the coupled BEM-GAs approach, showing its good performance for inverse analysis of CP systems.

2 Governing equation

Consider the problem of cathodic protection governed by the Laplace equation given by:

$$k\nabla^2 u = 0 \quad in\ \Omega, \tag{1}$$

where k is the conductivity of the electrolyte, u is the electrochemical potential and Ω is the domain.

The described problem is subjected to the following boundary conditions:

$$u = \bar{u} \quad on\ \ \Gamma_1, \tag{2a}$$

$$q = k\frac{\partial u}{\partial \boldsymbol{n}} = \bar{q} \quad on\ \Gamma_2, \tag{2b}$$

$$q = f(u) \quad on\ \Gamma_3, \tag{2c}$$

where $\Gamma = \Gamma_1 \cup \Gamma_2 \cup \Gamma_3$ is the boundary of Ω, q is the current density, **n** is the outward normal vector to the boundary Γ and $f(u)$ is a nonlinear function of u.

3 BEM and MFS formulations

Based on the direct formulation of the BEM, a weak form to the Laplace equation can be written as [18]:

$$c(\boldsymbol{\xi})u(\boldsymbol{\xi}) = \int_{\Gamma} u^*(\boldsymbol{\xi},\boldsymbol{x})q(\boldsymbol{x})d\Gamma(\boldsymbol{x}) - \int_{\Gamma} q^*(\boldsymbol{\xi},\boldsymbol{x})u(\boldsymbol{x})d\Gamma(\boldsymbol{x}), \tag{3}$$

where $u^*(\boldsymbol{\xi},\boldsymbol{x})$ and $q^*(\boldsymbol{\xi},\boldsymbol{x})$ define the fundamental solution for the potential and the current density, respectively.

The boundary must be discretized into elements, where the values of u and q can be constant on each element and a set of equations is obtained, i.e. $\mathbf{Hu} = \mathbf{Gp}$. This system is solved by imposing the boundary conditions. For the non-linear boundary condition, the Newton-Raphson method has been successfully used to solve the resulting non-linear system [19].

For the indirect BEM formulation, the contributions of **G** and **H** are uncoupled and the harmonic function u and its derivative in the direction of the outward normal to the boundary are given, after the discretization, by [18]:

$$u_i = \sum_{j=1}^{N} \sigma_j G_{ij}, \tag{4}$$

$$q_i = \sum_{j=1}^{N} \sigma_j H_{ij}, \tag{5}$$

where σ_j*'s* are the unknown values of the source intensities. Here, the diagonal terms in **H** are subtracted from -1 of the terms H_{ii} of the direct formulation. The Eqs. (4) and (5) can be applied at the boundary conditions to determine the source intensities.

A simpler procedure has been used to avoid the integrations of $u^*(\boldsymbol{\xi},\boldsymbol{x})$ and $q^*(\boldsymbol{\xi},\boldsymbol{x})$ over the boundary for the indirect BEM formulation. Since the superposition of fundamental solutions satisfies the Laplace equation when the source and field points are located at different positions and the boundary conditions can be imposed on a finite set of points on the boundary. This methodology is known as MFS. Usually, the source points (or virtual sources) are located outside the domain on a circular pseudo-boundary or on a line geometrically similar to the boundary. The number of virtual sources can be less than or equal to the number of boundary nodes. Thus, the source intensities (σ_j*'s*) need to be determined from a least square problem. To accommodate possible nonlinear boundary conditions, a modified version of the Levenberg-Marquardt algorithm [20] is used.

The anodes have been inserted as prescribed potential or source terms. In the last case, a function *b* arises in Laplace equation and the direct BEM results in the following equation:

$$c(\boldsymbol{\xi})u(\boldsymbol{\xi}) = \int_{\Gamma} u^*(\boldsymbol{\xi},\boldsymbol{x})q(\boldsymbol{x})d\Gamma(\boldsymbol{x}) - \int_{\boldsymbol{\Gamma}} q^*(\boldsymbol{\xi},\boldsymbol{x})u(\boldsymbol{x})d\Gamma(\boldsymbol{x}) + \int_{\Omega} b(\boldsymbol{x})u^*(\boldsymbol{\xi},\boldsymbol{x})d\Omega(\boldsymbol{x}), \tag{6}$$

The domain integral in Eq. (6) represents a particular solution for the non-homogenous partial differential equation, which involves a product of known functions. For general cases, it has been assumed that the source *b* can be approximated by Radial Basis functions (RBFs):

$$b(\boldsymbol{x}) \approx \hat{b}(\boldsymbol{x}) = \sum_{j=1}^{N+L} \Psi_j a_j, \tag{7}$$

with *N* being the number of boundary nodes, *L* the number of internal nodes and the a_j's are solved using the Eq. (7). Thus, an approximated particular solution can be written as ($\hat{u}_p \approx u_p$):

$$\hat{u}_p(\boldsymbol{x}) = \sum_{j=1}^{N+L} \Psi_j a_j, \tag{8}$$

where Ψ_j is obtained by analytical integration considering the radial part of Laplacian operator. Here, the Wendland RBF of compact support $\psi_j\left(\frac{r}{\beta}\right) = \left(1-\frac{r}{\beta}\right)^2$ is chosen and, after integration, Ψ_j has the following definition:

$$\Psi\left(\frac{r}{\beta}\right) = \begin{cases} \frac{r^4}{16\beta^2} - \frac{2r^3}{9\beta} + \frac{r^2}{4}, & r \le \beta \\ \frac{13\beta^2}{144} + \frac{\beta^2}{12} ln\left(\frac{r}{\beta}\right), & r > \beta \end{cases} \tag{9}$$

where β is the size of the support.

Numerical simulations are proposed considering direct BEM solution procedure (6) and the MFS combined with the method of particular solutions (MPS) [21], where the general solution (u) of the Poisson equation is divided into two parts, given by:

$$u(\boldsymbol{x}) = \int_{\Omega} b(\boldsymbol{x}) u^*(\boldsymbol{\xi}, \boldsymbol{x}) d\Omega + u_h(\boldsymbol{x}), \tag{10}$$

where $u_h(\mathbf{x})$ satisfies the Laplace equation and the corresponding boundary conditions.

4 MLPG2 formulation

The collocation method can be treated on the local weak form, where the test function over a sub-domain is Dirac's delta. This methodology is known as MLPG2 [14], and, using indicial notation, the global stiffness matrix $\boldsymbol{K}$ and the global load vector $\boldsymbol{f}$ are defined as:

$$K_{IJ} = \begin{cases} u^J_{,ii}(\boldsymbol{x}_I), & \boldsymbol{x}_I \in \Omega \\ u^J(\boldsymbol{x}_I), & \boldsymbol{x}_I \in \Gamma_u \\ u^J_{,n}(\boldsymbol{x}_I), & \boldsymbol{x}_I \in \Gamma_q \end{cases} \tag{11}$$

$$f_I = \begin{cases} b(\boldsymbol{x}_I), & \boldsymbol{x}_I \in \Omega \\ \bar{u}(\boldsymbol{x}_I), & \boldsymbol{x}_I \in \Gamma_u \\ \bar{q}(\boldsymbol{x}_I), & \boldsymbol{x}_I \in \Gamma_q, \end{cases} \tag{12}$$

with $I, J = 1, \dots, N + L$.

The trial function $u^t(\boldsymbol{x})$ in a domain of definition Ω_{x} can be written by:

$$u^t(\boldsymbol{x}) = \sum_{j=1}^{N_x} \phi_j(\boldsymbol{x}) \hat{u}_j(\boldsymbol{x}), \tag{13}$$

where $\phi_j(\mathbf{x})$ is the shape function of the Moving Least Square (MLS) approximation, $\hat{u}_j(\boldsymbol{x})$ is the fictitious nodal value and N_x is the number of the nodes in Ω_{x}.

Considering $\boldsymbol{p}^T(\mathbf{x}) = [p_1(\mathbf{x}), p_2(\mathbf{x}), \dots, p_m(\mathbf{x})]$ as complete monomial basis with m terms, the MLS shape function can be expressed as:

$$\phi_j(\boldsymbol{x}) = \sum_{i=1}^{m} p_i^T(\boldsymbol{x}) [\boldsymbol{A}^{-1}(\boldsymbol{x}) \boldsymbol{B}(\boldsymbol{x})]_{ij}, \tag{14}$$

where

$$\boldsymbol{A}(\boldsymbol{x}) = \sum_{j=1}^{N_x} w_j(\boldsymbol{x})\, \boldsymbol{p}_j(\boldsymbol{x}_j) \boldsymbol{p}_j^T(\boldsymbol{x}_j), \tag{15}$$

and

$$\boldsymbol{B}(\boldsymbol{x}) = [w_1(\boldsymbol{x}) \boldsymbol{p}(\boldsymbol{x}_1), w_2(\boldsymbol{x}) \boldsymbol{p}(\boldsymbol{x}_2), \dots, w_{N_x}(\boldsymbol{x}) \boldsymbol{p}(\boldsymbol{x}_{N_x})]. \tag{16}$$

In Eqs. (15) and (16) the 4th-order spline weight function (w_j) was considered, and the size of the support for the node x_j should be sufficiently large to ensure that $N_x > m$. The modified Levenberg-Marquardt method is also used to obtain the fictitious nodal values of the MLS approximation. Thus, these nodal values can be found to both the linear and nonlinear cases.

Two methodologies can be considered to deal with point sources. The first, the non-homogenous partial equation is solved using the MPS, as done with the MFS. The second, the normalized circular Gaussian function multiplied by intensity $P(\boldsymbol{x}'_g)$ is proposed to replace the point source:

$$b(\boldsymbol{x}) = \frac{P(\boldsymbol{x}'_g)}{2\pi\sigma^2} e^{-\frac{r_g^2}{2\sigma^2}}, \tag{17}$$

where σ is the standard deviation and r_g is the 2D Euclidean distance between $\boldsymbol{x}'_g$ and $\boldsymbol{x}$. Using the Gaussian function as source term, no particular solution needs to be known in the MLPG2 method. Analogous to the MFS, the solution of the MLPG2 method does not require numerical integration and

it is sensible to position of the collocation points. However, no second derivative is needed for the MFS.

5 Inverse problem

In this work, a mathematical function is presented as polarization curve model, where its parameters are explicitly related with the shape of the curve. Thus, the search range for the parameters can be appropriately chosen, and the convergence rate of the search algorithm increases. The smooth logistic sigmoid function is adapted by the van Genuchten-Mualem model [22] as:

$$u(q) = u_{cor} + \frac{u_e - u_{cor}}{(1+(\alpha q)^n)^{1-\frac{1}{n}}}, \tag{18}$$

where u_{cor}, u_e, α and n are parameters to be determined. The corrosion potential (u_{cor}) represents the open circuit potential at which the sum of the anodic and cathodic currents on the electrode surface is zero. The empirical parameter u_e represents the corresponding potential applied to the cathodic reaction. The constants α and n are the shape parameters of the polarization curve.

A genetic algorithm [23] is employed to minimize the objective function given by:

$$Z(c_j) = \sqrt{\frac{1}{M}\sum_{i=1}^{M}\left[u_{exp} - u_{num}^{i}(c_j)\right]^2}, \tag{19}$$

where *M* is the number of nodes that represent the boundary of the anode in the original problem, u_{exp} is the experimental value measured on the metal, $u_{num}(c_j)$ is the numerical value calculated on the metal for each c_j and c_j represents the parameters of the polarization curve with *j* being the number of generations to be provided by the GA.

6 Numerical results

The first example has the purpose of evaluating the MFS and MLPG2 methods for the problem of concentric circles of radius 10 cm and 5 cm. Two point sources were designed to protect the inner circle, where the following curve was prescribed as:

$$q(u) = 0.06 + 0.001\left(10^{\frac{-u-0.4}{0.2}} - 10^{\frac{u+0.1}{0.1}}\right), \tag{20}$$

where u and q have units V and mA/cm^2.

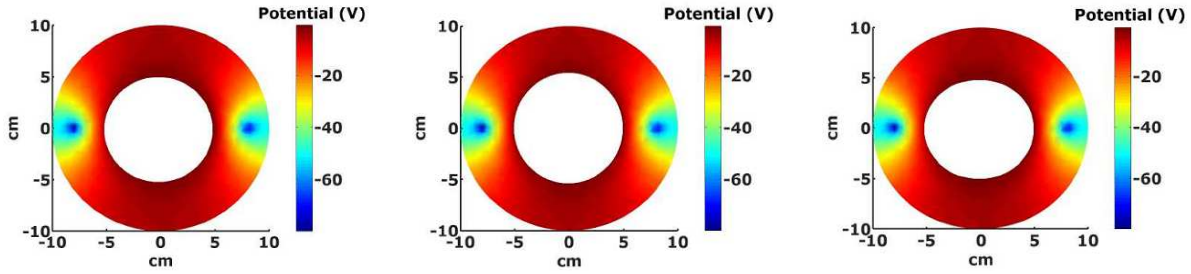

a) b) c)

Figure 1. Potential at the electrolyte using the numerical models: a) BEM, b) MFS and c) MLPG2.

In the outer circle, $q = 0\ mA/cm^2$ is prescribed. In this example, the conductivity of electrolyte is equal to $0.04\ \Omega^{-1}cm^{-1}$. The problem geometry was defined using 170 $(112 + 58)$ boundary nodes, 721 internal points and 168 $(112 + 56)$ virtual sources with optimum radius 12.22 cm and 2.94 cm. Each point source has intensity of $-4.5\ mA$, whose locations can be seen in Fig. 1. The solution provided by the MFS is presented in Fig. 2, whereas the MLPG2 solution can be observed in

Fig. 3. Analysis of these results shows that the three numerical methods present very similar results, thus revealing the good accuracy of the meshless methods.

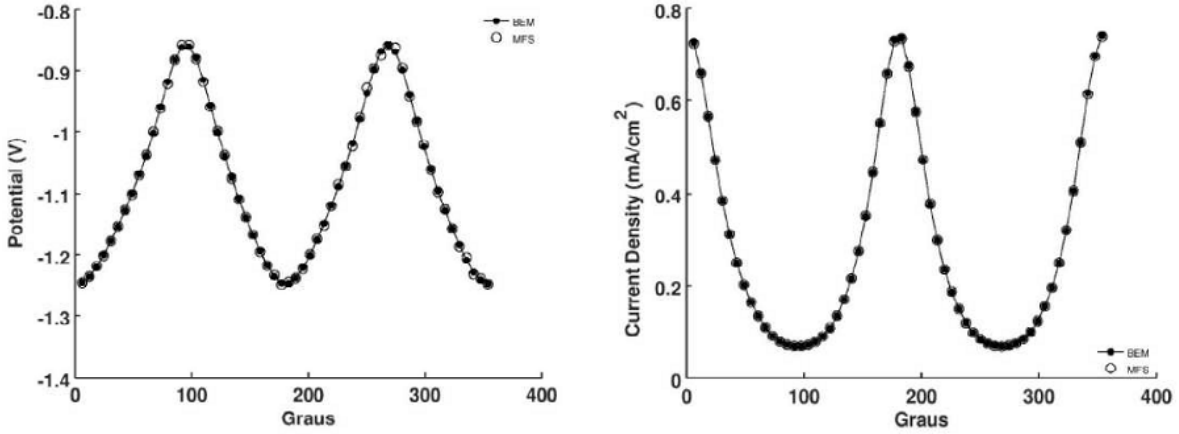

a) b)

Figure 3. Comparison of the BEM and MFS models: a) Potential distribution on the metal and b) Current density on the metal.

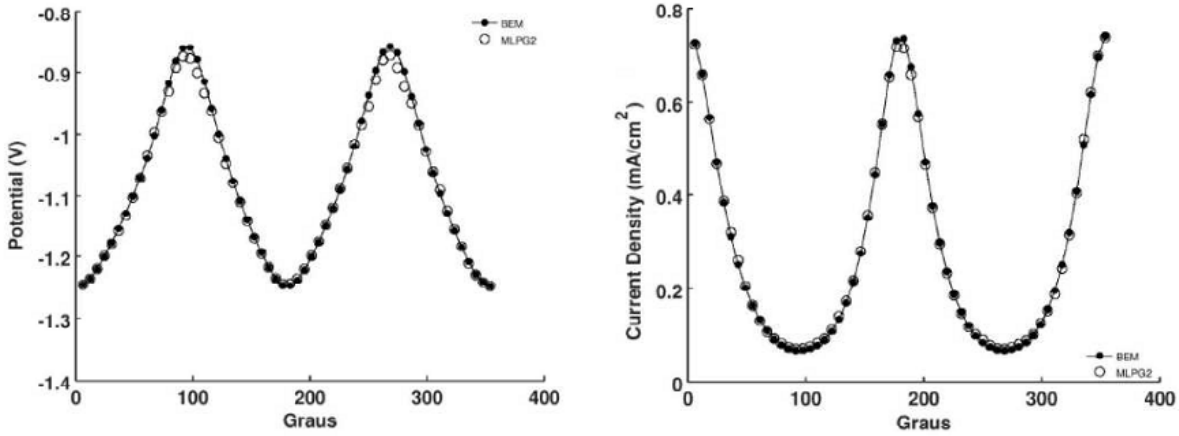

a) b)

Figure 3. Comparison of the BEM and MLPG2 models: a) Potential distribution on the metal and b) Current density on the metal.

In the next application, an inverse analysis to identify the polarization curve of a tank bottom is carried out. The conductivity of electrolyte is equal to $1.0\ \Omega^{-1}cm^{-1}$. The tank has $20\ m$ of radius (R) and seven anodes (line sources) were inserted between the tank bottom and the liner, as shown in Fig. 4. The total impressed current is equal to $-0.35\ A/m^2$.

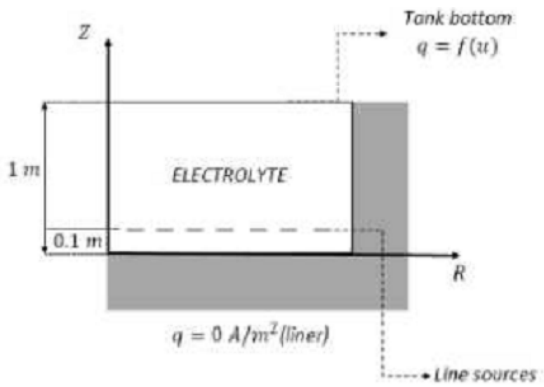

Figure 4. The axisymmetric problem.

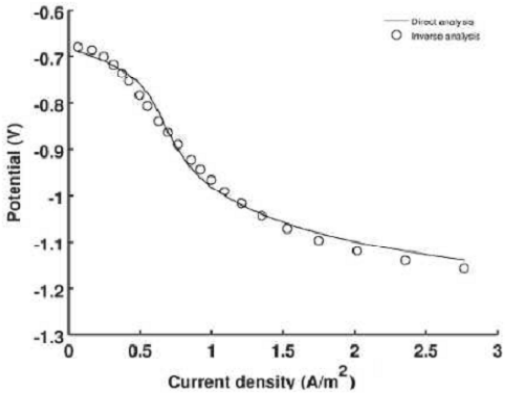

Figure 5. Polarization curves.

The direct problem is solved by using BEM with 290 boundary nodes. In this model, the axisymmetric fundamental solution for Laplace's equation is applied. The polarization curve (Eq. (18)) is, firstly, used to calculate the potential values over the tank bottom, at the positions $R = 1.0$, 3.0, 5.0, 10.0 and 18.0 m. The potential values obtained by BEM model were $-1.225\,V$, $-0.978\,V$, $-0.839\,V$, $-0.738\,V$ and $-0.699\,V$. Thus, the GA was used to minimize the objective function (Eq. (19)) in order to obtain the design variables u_{cor}, u_e, α and n. The range of these parameters is assumed to be $[-0.7, -0.1]$, $[-1.5, -0.7]$, [0.5,10.0] and $[-2.0, -0.1]$. In the 99^{th} generation, the GA provided $u_{cor} = -0.680\,V$, $u_e = -1.209\,V$, $\alpha = 1.434 m^2/A$ and $n = -1.922$ ($Z(c_{99}) = 10^{-4}$). Fig. 5 shows the real polarization curve and the estimated values using the optimum parameters provided by the proposed approach. Analysis of these results clearly confirms that there is a good agreement among the two curves.

7 Concluding Remarks

In this paper, truly meshless methods (MFS and MLPG2) and the direct BEM solution procedure have been applied to classical two-dimensional corrosion engineering problems. The proposed methods were successfully introduced and its results were validated using BEM results. In the main example, a sigmoid function was typically adopted for the modeling of the polarization curve, considering a practical axisymmetric problem. The parameters of the proposed model were obtained through the potential values experimentally measured on the metal surface and the GA coupled with the BEM.

Variants of the MLPG method will be the subject of future publications. The authors believe that the MLPG4 (also known as local boundary integral equation) and the MLPG5 (where the test function is the Heaviside step function) are great promises to compete with the BEM as a method of choice in numerical simulations of CP systems.

Acknowledgements

The authors acknowledge the financial support of Conselho Nacional de Desenvolvimento Científico e Tecnológico (CNPq). This study was also financed in part by the Coordenação de Aperfeiçoamento de Pessoal de Nível Superior – Brasil (CAPES) – Finance Code 001.

References

[1] V. Cicek. *Cathodic Protection: Industrial Solutions for Protecting Against Corrosion*, John Wiley & Sons Inc, New York, United States, 2013.

[2] R. N. Fleck. *Numerical evaluation of current distribution in electrical systems*, Master's thesis, University of California, 1964.

[3] P. Doig and P. E. J. Flewitt. A finite difference numerical analysis of galvanic corrosion for semi-infinite linear coplanar electrodes, *Journal of the Electrochemical Society*, vol. 12, pp. 2057-2063, 1979.
[4] J. W. Fu. A finite element analysis of corrosion cells, *Corrosion/NACE*, vol. 38, n. 5, pp. 9-12 1982.
[5] R. Montoya, O. Rendon and J. Genesca. Mathematical simulation of cathodic protection system by finite element method, *Materials and Corrosion*, vol. 56, pp. 404-411, 2005.
[6] A. H. D. Cheng and D. T. Cheng. Heritage and early history of the boundary element method, *Engineering Analysis with Boundary Elements*, vol. 29, pp. 268-302, 2005.
[7] C. A. Brebbia, The birth of the boundary element method from conception to application, *Engineering Analysis with Boundary Elements*, vol. 77, pp. xx-xx, 2017.
[8] J. C. F. Telles, W. J. Mansur, L. C. Wrobel and M. G. Marinho. Numerical Simulation of a Cathodically Protected Semisubmersible Platform using PROCAT System, *Corrosion*, vol. 46, pp. 513-518, 1990.
[9] S. L. D. C. Brasil, J. C. F. Telles and L. R. M. Miranda. On the effect of some critical parameters in cathodic protection systems: A numerical/experimental study, *Computer Modeling in Corrosion, ASTM STP 1154, R.S. Munn Ed., American Society for Testing and Materials*, vol. 380, pp. 277-291 1991.
[10] J. A. F. Santiago and J. C. F. Telles. On Boundary Elements for Simulation of Cathodic Protection Systems with Dynamic Polarization Curves, *International Journal for Numerical Methods in Engineering*, vol. 40, pp. 2611-2622, 1997.
[11] W. J. Santos, S. L. D. C. Brasil, J. A. F. Santiago and J. C. F. Telles. A new solution technique for cathodic protection systems with homogeneous region by the boundary element method, *European Journal of Computational Mechanics*, vol. 1, pp. 1-15, 2018.
[12] V. D. Kupradze and M. A. Aleksidze. Aproximate method of solving certain boundary-value problems, *Soobshch akad nauk Gruz SSR*, vol. 30, pp. 529-536, 1963.
[13] W. J. Santos, J. A. F. Santiago and J. C. F Telles. An Application of Genetic Algorithms and the Method of Fundamental Solutions to Simulate Cathodic Protection Systems, *Computer Modeling in Engineering & Sciences*, vol. 87, pp. 23-40, 2012.
[14] S. N. Atluri and S. Shen. The meshless local Petrov-Galerkin (MLPG) method: A simple & less-costly alternative to the finite element and boundary element methods, *Computer Modeling in Engineering & Sciences*, vol. 34, pp. 11-51, 2002.
[15] E. F. Fontes, J. A. F. Santiago and J. C. F. Telles. An iterative coupling between meshless methods to solve embedded crack problems, *Engineering Analysis with Boundary Elements*, vol. 55, pp. 52-57, 2015.
[16] M. Barbosa, E. F. Fontes, J. C. F. Telles and W. J. Santos. An efficient hybrid implementation of MLPG method, *Journal of Multiscale Modelling*, vol. 8, pp. 1740002 (11 pages), 2017.
[17] D. H. Konda, J. A. F. Santiago, J. C. F. Telles, J. P. F. Mello and E. G. A. Costa. A meshless reissner plate bending procedure using local radial point interpolation with an efficient integration scheme, *Engineering Analysis with Boundary Elements*, vol. 99, pp. 46-59, 2019.
[18] C. A. Brebbia, J. C. F. Telles and L. C. Wrobel. *Boundary Element Techniques: Theory and Applications in Engineering*, Springer, Berlin, 1984.
[19] J. P. S. Azevedo and L. C. Wrobel. Nonlinear heat conduction in composite bodies: a boundary element formulation, *International Journal for Numerical Methods in Engineering*, vol. 26, pp. 19-38, 1988.
[20] W. J. Santos, J. A. F. Santiago and J. C. F Telles. Optimal positioning of anodes and virtual sources in the design of cathodic protection systems using the method of fundamental solutions, *Engineering Analysis with Boundary Elements*, vol. 46, pp. 67-74, 2014.
[21] W. J. Santos, J. A. F. Santiago and J. C. F Telles. Using the Gaussian function to simulate constant potential anodes in multiobjective optimization of cathodic protection systems, *Engineering Analysis with Boundary Elements*, vol. 73, pp. 35-41, 2016.
[22] M. T. van Genuchten. A closed-form equation for predicting the hydraulic conductivity of unsaturated soils, *Soil Science Society of America Journal*, vol. 44, pp. 892-898, 1980.
[23] Z. Michalewicz. *Genetic Algorithms + Data Structures = Evolution Programs*, Spinger-Verlag, 1996.